

**AJMHR**

Asian Journal of Medical and Health Research

Journal home page: www.ajmhr.com

A Review of Coded Aperture Families having Perfect Mathematical Imaging Properties used for Near Field Imaging Application

M. A. Alnafea*Department of Radiological Sciences, King Saud University, Riyadh, Saudi Arabia*

ABSTRACT

The pinhole camera is a well-established direct-imaging system that produce good quality images, in terms of spatial resolution, but has an associated limited field of view. When used in the context of nuclear medicine imaging, the limited angular acceptance and poor geometric efficiency means the imaging process suffers from lengthy acquisition times as it suffers from low efficiency due to its single small pinhole size. The collimator image formation such as the parallel-hole is limited by the design and also provides a low detection efficiency. The forthcoming review focuses on methods of removing these limitations by investigation using a Coded Aperture (CA) instead of a conventional collimator, coupled to a standard clinical gamma camera for breast tumour imaging applications. This paper introduces the concept of CA imaging and provides an historical background of the different types of CA, families with their mathematical imaging properties. Then, it describes their shape and correlation properties. These include Fresnel zone plate, random array, non-redundant arrays, L shape geometric array, X shape geometric, uniformly redundant, modified uniformly redundant, mosaic uniformly redundant and no-Two-Hole-Touching patterns. Finally, this paper illustrating the principle of pinhole camera to appreciate the theory and the formation of coded image. Then describe the potential of CA imaging in breast tumour imaging. It a general overview of the entire imaging problems associated with the collimator-based SM system closes the paper.

Keywords: Coded Aperture, Pinhole Camera, Coded Image

*Corresponding Author Email: alnafea@ksu.edu.sa

Received 07 July 2018, Accepted 23 July 2018

Please cite this article as: Alnafea MA., *A Review of Coded Aperture Families having Perfect Mathematical Imaging Properties used for Near Field Imaging Application*. Asian Journal of Medical and Health Research 2017.

INTRODUCTION

Imaging with gamma rays needs a form of geometrical collimator such as a pinhole. As shown in Fig.1(a) the gamma flux passes through a hole in an opaque plate so that an image is formed in a position sensitive detector. This gives images with excellent intrinsic spatial resolution, but due to its small hole size results, results in extremely poor efficiency. Thus, gamma cameras with many pinholes (Fig.1(b)) have been used as a solution to obtain a much larger fraction of the incident flux whilst preserving the high spatial resolution properties of a single pin hole design. The image produced from such camera is based on the principle of "Spatial Signal Multiplexing" [1]. This simply means that every incident photon impinging on the detector, within the object Field Of View (FoV), participates in encoding the flux into a predetermined pattern or code, thus called Coded Aperture (CA) or mask. This process casts a shadow of the encoding pattern onto the detector surface. To obtain a useful image, the encoded pattern (projected image) may then be decoded, by a variety of methods, but most commonly by using the correlation analysis of the pattern produced by a point source.

Coded Image Formation

Anger cameras use a collimator to form a projected image of the incident photon flux. This is achieved by geometrically rejecting photons with oblique incidence, and only permitting photons with a narrow range of incident directions to reach the detector surface. By contrast, CA imaging systems generally accept a much larger fraction of the incident photon flux and encode the flux into a predetermined pattern or code, which then casts a shadow of this pattern onto the detector surface. For instance, when imaging a point source (with low statistical noise), in the far-field geometry, then each photon contributes to casting a shadow (encoded flux) of part of the aperture pattern onto the detector surface. This means that the counts of the point source spread over a non-point like surface area. The size or magnification of the aperture shadow depends on the distance of the point source from the CA only in near field application. To obtain a useful image, the encoded pattern is then decoded, most often by using the correlation of the observed pattern with a suitable decoding function. In the case of imaging an extended object the basic concept does not change. Each point in the object can be regarded as a point source casting an aperture shadow of a certain size and location on the detector. In other words, the number of photons passing through a single hole of the CA is independent of photons passing through all other aperture holes. The contributions from each aperture hole represent the total projections of the object being imaged. These projections, collected at the detector, are composed of many shifted copies of the source object. The decoding process can be obtained in a similar way as in the case of point source. As CAs

have been historically developed for far_field imaging applications, then the behavior of CAs in this geometry will be discussed initially.

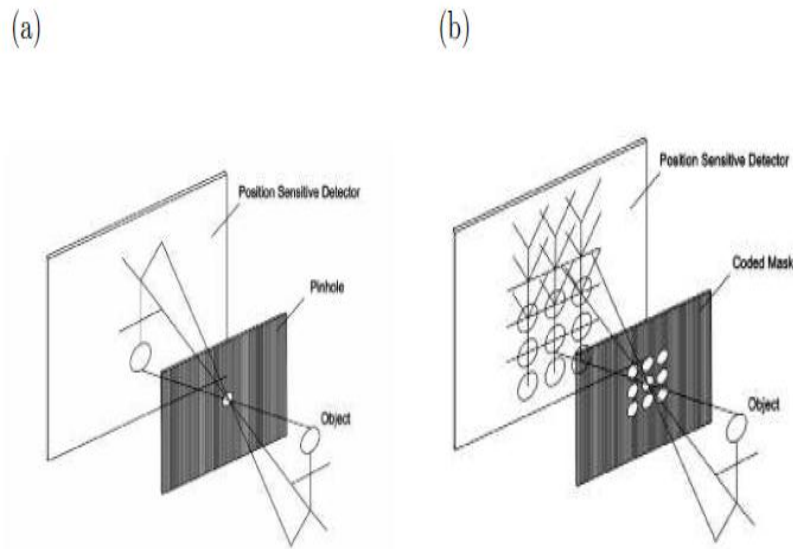


Figure 1: Schematic diagrams of two image formation principles: (a) a pinhole camera, (b) multiple pinholes camera (CA mask). Note: both techniques gives inverted image of the object.

Following Fenimore [16] for an object denoted by array O located at infinity from the aperture pattern, that is defined by the array A (a 2D function containing a 0 where the aperture is closed, and 1 where it contains a hole), and given a noise term denoted by an array B then the recorded image, D , can be given as in Equation 1:

$$D = (O * A) + B \quad (1)$$

where: $*$, is the convolution operator and is used here because the process is physical. As most aperture arrays have a large number of holes, D does not look like O at all. In other words, a point in the image is not represented on the detector by a point, but rather by the shadow of the mask pattern or part of it (see Fig. 2). This is what basically causes the signal or the information of the source to be encoded. In this sense the point source is not counted once, but once for every hole of the CA. This can be expected to increase the counting statistics in the image D , and consequently, the quality of the image. On the other hand, on imaging an extended source object or many point sources, the source spatial information is then multiplexed. This is because each detector element receives as much information (signal) as the number of point sources incident on it. The recorded (projected) pattern, D , must be decoded to recover the source object information and obtain a useful image. In other words, D must be scanned or correlated with the known pattern array to replace the shadow gram cast by a point source in order to separate the overlapped copies cast by an extended

source object. The reconstructed image, (I), in the proposed patterns, is often obtained by correlating D with a post processing array, G (inverse filter of A), and is defined as:

$$I = D \otimes G \quad (2)$$

where: \otimes , indicates periodic correlation.

The particular imaging properties of these patterns is that given arrays A and G then $(A \otimes G)$ approximates a δ function. The G function is obtained using the balanced correlation method [2] that contains 1 where there is a hole and -1 where it is closed. Using Eq.1 but ignoring the noise term, I can be written as:

$$I = D \otimes G = O * (A \otimes G) \quad (3)$$

This suggests that the correlation of the projected image with the post-processing array is just the original image plus, of course, the ignored noise term. The quality of the object reconstruction therefore depends on the choice of the aperture A and the decoding function G [2,3]. If G can be chosen so that:

$$A \otimes G = \delta \quad (4)$$

In this case Eq. 3 can be reduced to the convolution:

$$I = O * \delta = O \quad (5)$$

This indicates that the reconstructed image will perfectly represent the object (i.e. $I \approx O$). From the above equations one can infer that the final output of the CA imaging system is not directly the object but a convolution of the object with the system response or $(A \otimes G)$. This is referred as the system Point Spread Function (PSF) i.e. the image produced in response to a point source. From this definition, Eq. 5 becomes:

$$I = O * \text{PSF} \quad (6)$$

Thus, for a single point, then:

$$I = \delta * \text{PSF} = \text{PSF} \quad (7)$$

This suggests that a properly designed CA imaging system should spread (blur) the point over a very small area of the detector. Thus, the PSF clearly describes the behavior of the imaging system. This is because the output of the imaging system can be predicted by knowing both the input and the system PSF. Thus, in CA imaging the system PSF can be described by the convolution of the arrays A and G:

$$\text{PSF} = (A \otimes G) \quad (8)$$

From the above if the correlation of A and G i.e. the PSF gives a δ function then the construction is perfect. There are many types of arrays proposed in the literature that their generation of A and G satisfy the condition $A \otimes G \approx \delta$. Having demonstrated the CA image formation principle in simple terms more details of the fundamentals of CA imaging are given here. The basic mathematical formulation that describes the formation of the coded

image when imaging a planar source is summarized below based on analysis in [4]. For simplicity, let us consider imaging a point source with a simple pinhole (one pixel) as illustrated in Fig. 3 (a). The recorded counts of photons from that point source in one detector pixel (assuming $a=b$ and thus, the pixel size at the detector plane is twice the pixel size mask opening).

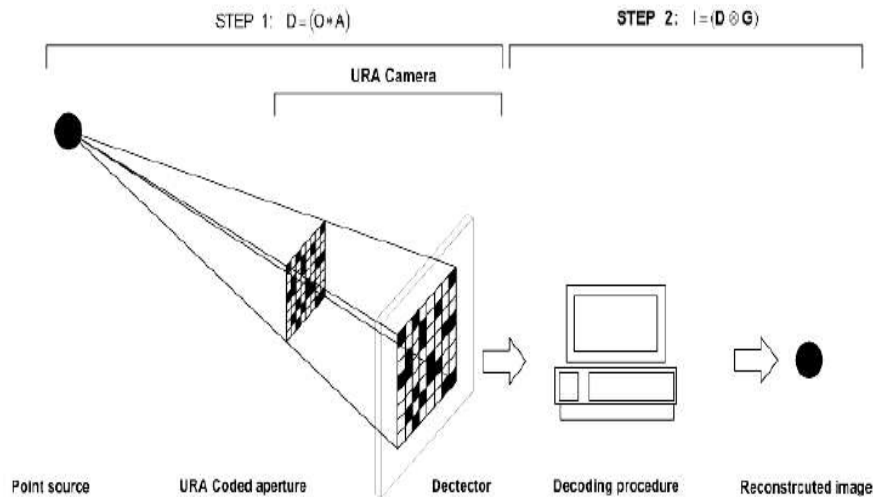


Figure 2: A schematic diagram of coded aperture principle imaging a point source.

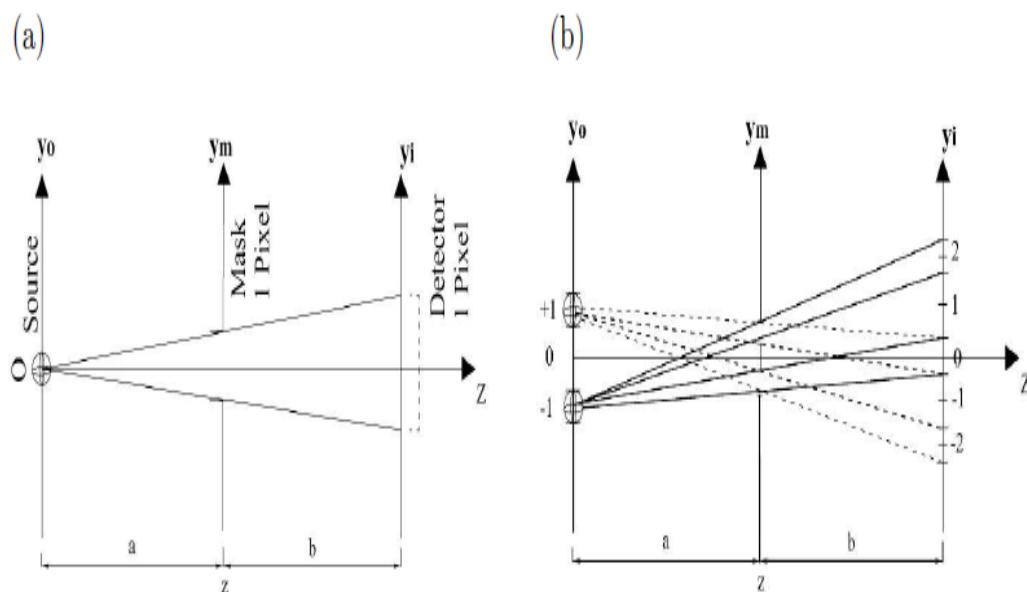


Figure 3. Schematic representation of projection geometry: (a) pinhole (one single hole of the mask) geometry demonstrating that $D(y_i = 0) = O(y_0 = 0) \times \Omega$ and zero elsewhere, (b) consider two open hole geometry at y_i with the first hole at 0.5 and the second at -0.5, note that y_0 is the coordinate of the source at the source axis and y_i is the coordinate of the detector pixel.

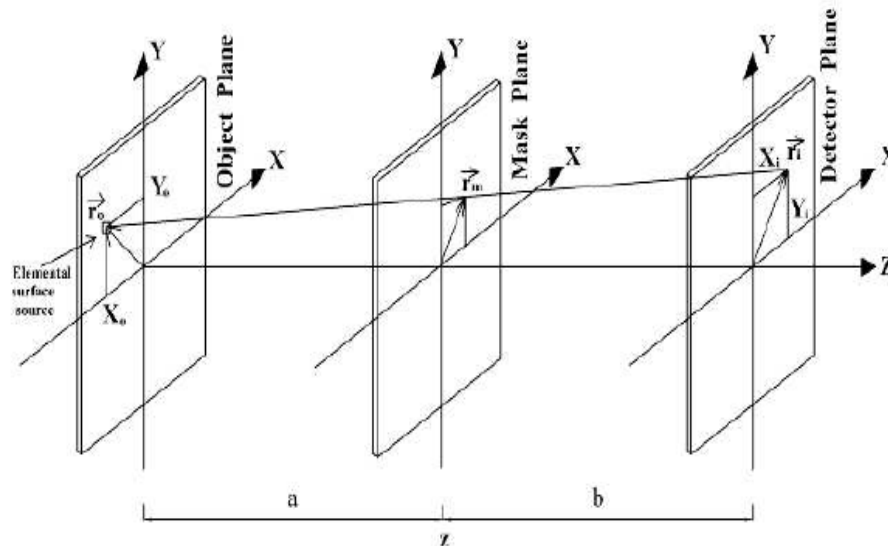


Figure 4. A schematic representation of the coded aperture geometry showing the point of intersection with the ray going from \vec{r}_0 to \vec{r}_i . Adapted from [4].

Where: (a) is the distance between the source and the mask, (b) is the distance between the mask and the detector, (Ω) is the solid angle) is given by:

$$D(y_i = 0) = O(y_0 = 0) \times \Omega \quad (9)$$

Now consider the case of two pinholes (at y_m that illustrated in Fig. 3 (b) the recorded counts in each detector pixels at the centre of y_i are given by:

$$D(y_i = 0) = O_1 \times \Omega (\text{pinhole 1}) + O_2 \times \Omega (\text{pinhole 2})$$

$$D(y_i = 1) = 0$$

$$D(y_i = -1) = 0$$

$$D(y_i = 2) = O_2 \times \Omega (\text{pinhole 1})$$

$$D(y_i = -2) = O_1 \times \Omega (\text{pinhole 2}) \quad (10)$$

Equation 10 can be generalized as:

$$D(y_i) = \sum_{s=1}^{S1} o_s A(y_m) \Omega(y_0, y_m) \quad (11)$$

where $S1$ is the number sources, $A(y_m)$ is the mask opening when a ray is drawn from y_0 to y_i and intercept the mask plane at y_m . Let us take this example with $y_0 = -1$ and $y_i = 2$ the ray pass through pinhole 1 at 0.5 with reference to Fig. 3 (b) $y_m = 1/2 (y_0 + y_i) = 0.5$.

Now consider the case of a 2D source emitting at distance Z from the detector, and encoded by a CA placed at distance b from the detector. The 2D planar source object, at distance, $a=(Z-b)$, from the CA, is denoted by O . The aperture pattern is given by the array A (a 2D function containing a 0 where the aperture is closed, and 1 where it contains a hole). Finally the noise is

denoted by array B (noise term) but is initially ignored here to simplify the analysis. With reference to Fig. 4 the elemental distribution of the recorded counts in the detector at position \vec{r}_i , is represented by $dD(\vec{r}_i)$ such as:

$$dD(\vec{r}_i) = O(\vec{r}_o)A(\vec{r}_m)\Omega(\vec{r}_o, \vec{r}_m)d^2(\vec{r}_o) \quad (12)$$

where $O(\vec{r}_o)d^2(\vec{r}_o)$ is the intensity of the elemental 2D source at \vec{r}_o .

The above equation suggest that the photon distribution from the object \vec{r}_o recorded at the detector in position \vec{r}_i is modulated by the mask. With $\vec{r}_m = \vec{r}_i + (\vec{r}_i - \vec{r}_o) a/Z$ and it is the vector represent the intersection of the ray going from \vec{r}_o to \vec{r}_i with the mask plane.

To obtain the total photon distribution recorded at the detector we need to integrate over the object plane as:

$$dD(\vec{r}_i) = \iint O(\vec{r}_o)A\left(\frac{a}{Z}\vec{r}_i + \frac{b}{Z}\vec{r}_o\right)\Omega(\vec{r}_o, \vec{r}_m)d^2(\vec{r}_o) \quad (13)$$

where:

$$\Omega(\vec{r}_o, \vec{r}_m) = \frac{p_m^2}{a^2} \cos^3(\theta) \quad (14)$$

where $\theta = \tan^{-1}(|\vec{r}_i - \vec{r}_o|/z)$ and p_m is the mask pixel size.

The above geometric theory suggest that it is possible to calculate the projection from any aperture and object based on purely geometrical calculations. It also demonstrates that the photon distribution D recorded at the detector position \vec{r}_i and due to the point source at \vec{r}_o is equal to the source $O(\vec{r}_o)$, modulated by the mask transmission A. In far_field geometry $\cos^3(\theta) \cong 1$.

Ease of Use OVERVIEW OF THE VARIOUS FORMS OF CA PATTERNS

The first form of a viable CA pattern was proposed by Mertz and Young [5] for imaging faint stars in astronomy. In such imaging applications, the problem is characterized by far field geometry i.e. the objects are located at infinity from the detector. In this case all the incident photons travel in nearly straight lines (parallel to each other) and fall perpendicular to the imaging detector. In the early days of this application, the Fresnel Zone Plate (FZP) pattern [5] was the most widely used CA design.

As demonstrated in Fig.5, the FZP consists of a series of circular patterns of equal area arranged in an alternating design. One half of its area is open (transparent) and the other is closed (opaque) to γ -rays.

The large open area means that photons at a wide variety of angles may be accepted giving more depth information and thus, 3D information of the source position. It also means that such patterns possess a higher sensitivity than collimator based-systems as there is a far

greater open area. Consequently, this approach was applied in the medical γ -ray imaging domain by Barrett [7] as an alternative to the pinhole collimator. A considerable amount of clinical work was followed by Rogers and colleague [8]. However, it has been reported [6,9] that the FZP is not ideal in its imaging properties. This is because the auto-correlation function of such patterns have side lobes artefacts and its Fourier transform is not perfectly flat. It also possesses a poor resolution that limits its wide acceptance [6].

The random pattern [10,11] (see Fig. 6 (a)) is also one of the early CA that has been proposed as an extension of the pinhole camera. The idea behind the random array is to increase the open area of the mask, while preserving its spatial resolution. The detection efficiency may further be increased by enlarging the mask hole size, but this will be at the cost of the resolution. The random character is necessary to get imaging properties that approximate a δ auto-correlation function. However, it has been reported [6,12] that the random arrays suffer from inherent noise due to the presence of side-lobes as demonstrate in Fig.6(b).

Soon after various alternative design patterns have been proposed with the hope to maximize the detection efficiency without degrading the resolution. For instance, in 1971 Non Redundant Arrays (NRAs) [13] were introduced as an extension of the pinhole camera. As shown in Fig. 7(a) this type of CA is made up of small pinholes arranged in a non-redundant pattern i.e. with no repetition of the hole pattern present [13]. In other words, the spacing between any two holes occurs only once over the whole aperture plane. These arrays are compact and have nearly perfect imaging characteristics, but only on a very small FoV. However, its small number of holes prevent great improvements in the detection efficiency.

Then ten years later, time modulated CAs have been developed to eliminate some of the problems of the stationary CAs. The main principle is that the γ -ray transmission at different points in the aperture varied independently. Several other approaches have been proposed for instance the rotating slit suggested by Tanaka and Linuma [6] and the stochastic aperture proposed by May [6]. The former consists of a small transparent slit rotating about its centre but the latter is more sophisticated. This is because the aperture used for imaging is stepped through a sequence of positions so that all the elements are cyclic in the time domain.

The most promising time coded aperture is the planar pseudo random binary sequence also called stochastic time modulated CAs. This is because during scanning the CAs is stationary but its elements CAs are cyclically permuted for each subinterval of the scan. This allows image decoding to be performed on a detector element by element basis.

Figure 8 illustrates a simple geometry of a stochastic time modulated CAs, the imaging principle of such CAs, using a single point source, is that as the aperture is moved in its plane the detector record the signal of the source. The aperture movement is through a sequence of

positions encoded (in the time domain) the signal of the source as the phase or time is different. A simple correlation analysis with a suitable decoding function is needed to recover the source information. The use of array of detectors as shown in Fig. 8 permits tomographic imaging for instance, the first detector records the same signal from sources number 1 and 3. In addition, point 1 and 3 have different positions and are projected to detector 4 and thus viewed from different angle. This permits tomographic imaging and the use of an array of detectors that makes the design simpler.

In 1983 Gourelary [14-16] introduced several new geometrical arrays. These arrays are flexible in their designs and having open fraction less than 50%. The main designs focus on L and X family arrays having a square shape, where L shape mean that the open hole has L shape and X shape mean that the open hole has X shape Two examples of these arrays are shown in Fig. 9 for the L family and Fig. 10 for the X family. Unfortunately, these arrays do not provide any advantages over the aforementioned patterns. The imaging performance of these arrays depends on the location of the object within the FoV [14-16]. This may be because these geometric arrays are not cyclic in its nature.

The majority of the above CAs approaches are impractical and are rarely used in clinical practice. This is because the autocorrelation functions in these array are subject to coding noise or artefacts [12]. Some of these patterns had been successfully used, and continue to be used, in the astrophysical field but, to date, have not achieved great success in the medical imaging domain.

Many of the inherent drawbacks of the above patterns were overcome in 1977, when Fenimore [3] introduced the rectangular Uniformly Redundant Arrays (URAs), which has several attractive imaging properties flat, has delta function and side lobe (as demonstrated in Fig. 11) and are finite. These arrays have rapidly gained a wide spread acceptance in the field of astronomy. A decade later, URAs were followed by the Modified URAs (MURAs) (see Fig. 12) [17]. From the URAs and MURAs one can construct a self-supporting array called No-Two-Hole-Touching design(as shown in Fig. 13).

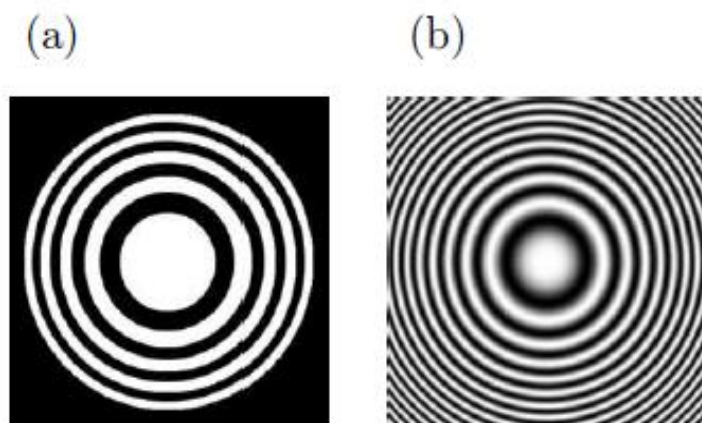


Figure 5. The FZP Coded Aperture patterns [6]: (a) a binary FZP, (b) a sinusoidal zone plate that has infinite extent. The resulting image from such pattern is a hologram that can also be reconstructed with coherent optical system.

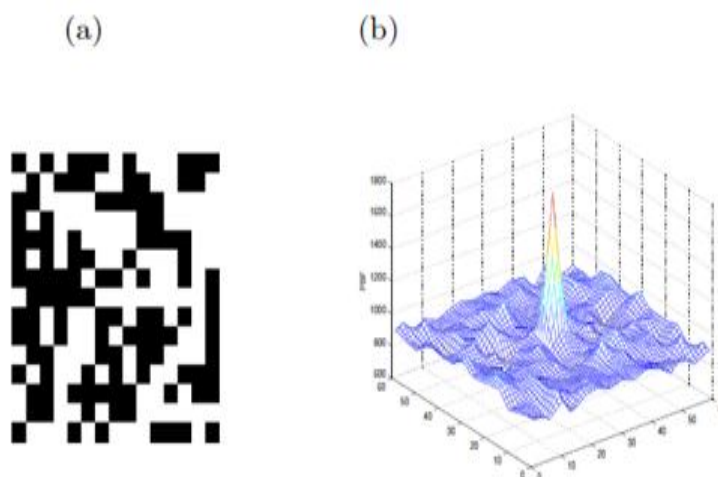


Figure 6. An example of a random array and its auto-correlation response function: (a) a random binary mask of size 15×15 , (b) 3D plot of the array auto-correlated image showing a peak on top of a ‘lumpy’ correlation background with the ratio between the two equal to the open fraction.

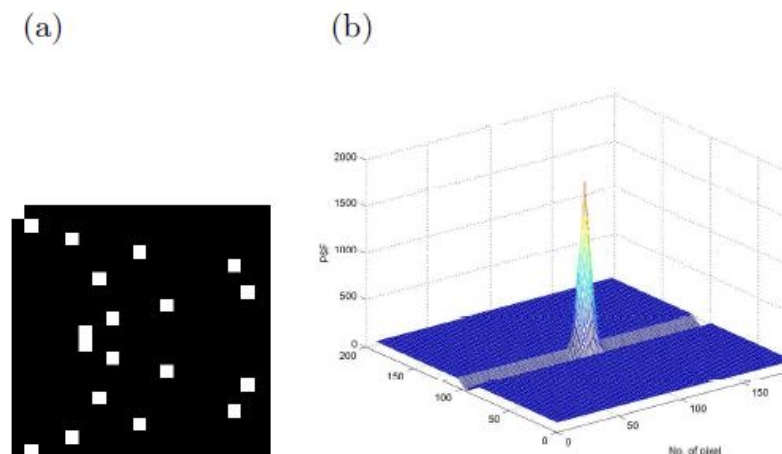


Figure 7. The non-redundant array and its response function: (a) a non-redundant binary array of 19×19 elements, (b) a 3D plot of its auto-correlation function clearly demonstrating the non-ideal imaging properties.

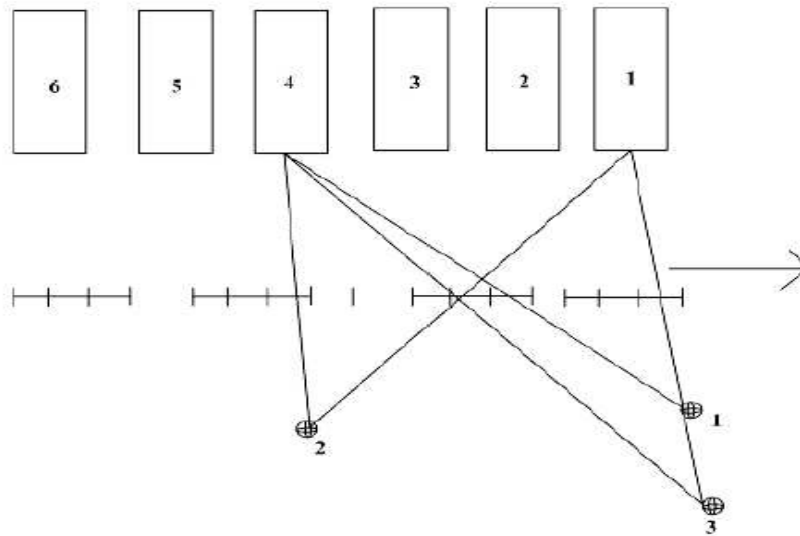


Figure 8. Simple geometry illustrating 1D pseudo-random sequence time-modulated coded aperture. Figure adapted and redrawn from [6].

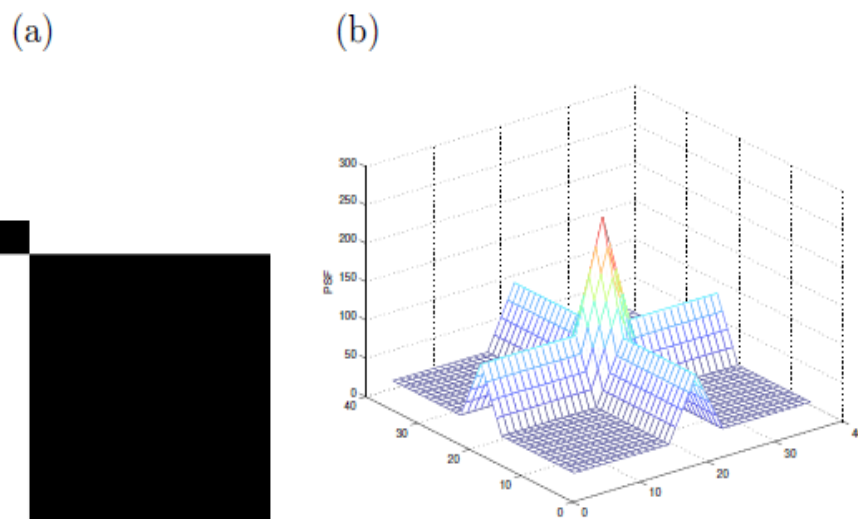


Figure 9. The L shape geometric array and its response function: (a) a geometric array of 9×9 elements, (b) a 3D plot of its auto-correlation function clearly demonstrating the non-ideal imaging properties.

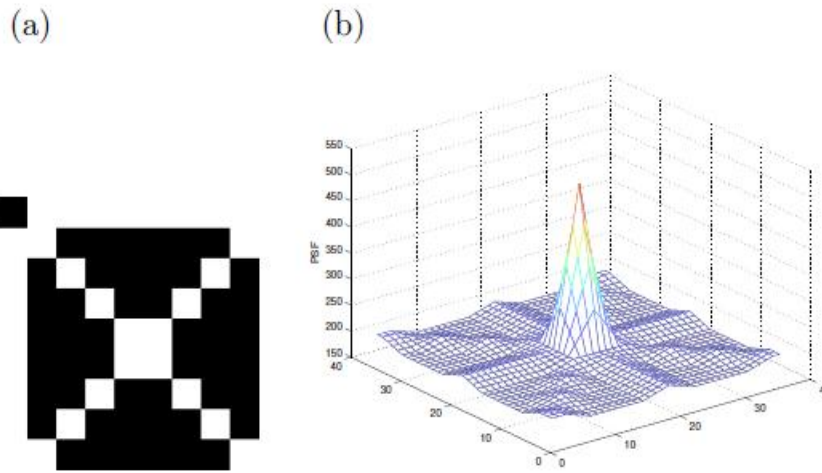


Figure 10. The X shape geometric array and its response function: (a) a geometric array of 9×9 elements, (b) a 3D plot of its auto-correlation function clearly demonstrating side-lobes in the image.

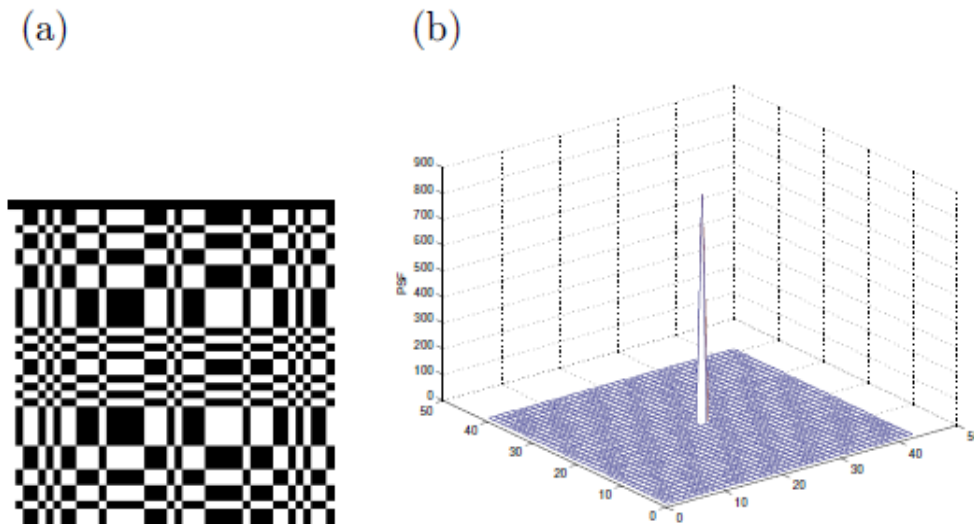


Figure 11. Binary URA mask and its correlation PSF: (a) 43×41 pattern where white corresponds to 1 and black corresponds to 0, (b) The correlation function of URA.

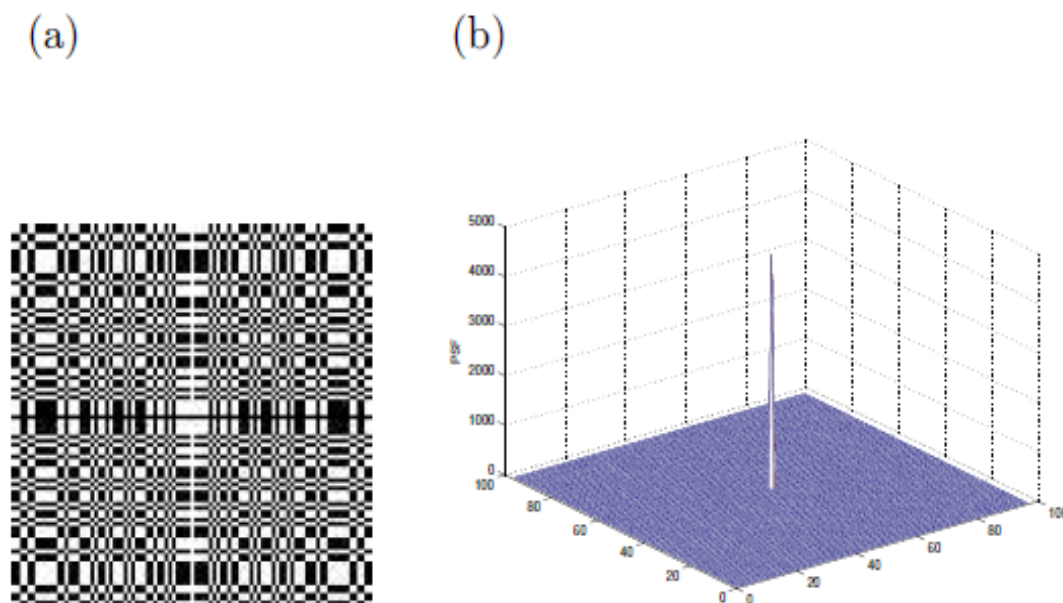


Figure 12. Binary MURA mask and its correlation PSF: (a) 97×97 pattern where white corresponds to 1 and black corresponds to 0, (b) The correlation function of the MURA. Such arrays also having perfect correlation property providing a δ -like impulse response function for the imaging system.

POTENTIAL FOR CA IMAGING IN BREAST CANCER DETECTION

The early proposed CAs imaging techniques such as the FZP [5] and the random array [10, 11] have been avoided because it suffers to some degree from distortion artefacts. Thus, it has been shown by [6, 21] that these patterns fail to deliver superior results compared to collimators and pinhole camera systems. However, the development of CA patterns based on "Cyclic Difference Sets" such as URAs MURAs and arrays based on MURAs such as NTHIT [2,3,17,22] have been demonstrated to be the most promising of all the CA patterns. These optimum arrays, as originally developed and extended by Fenimore and Cannon [2,3,25,26] have become widely used in the detection of X-ray and gamma-ray sources in astronomy for imaging stars and more recently in nuclear medicine for small animal imaging [18].

These arrays combine the high transmission (have up to 50% open area for the MURA patterns) characteristic with flat (zero) side-lobes in their response function. The high transmission provides a potential capability to image low-contrast sources and may dramatically enhances the detection efficiency compared to collimators system. These patterns have an interesting property that one can generate the mask and its negative (anti-mask) along with the decoding patterns, G , for each one. Two separate images can be then taken one with the mask and the second with the anti-mask and then add these two images after decoding each projected image with its post-processing decoding array. This technique

is of special interest in artefact reduction and has been used in the past for reducing systemic non-uniform background [27]. Certainly, these advantages and properties have motivated the authors to select this family of CA patterns as appropriate for use in SM.

Over 15 years a number of attempts have been made to use URA-CAs for 3D (SPECT and PET) imaging e.g. [28,29]. They have demonstrated that the use of URAs have improved sensitivity and resolution over single pinhole collimators. However, their resolution does not exceed that of planar parallel-hole collimators and this may be due to the complexity of the reconstruction or convolution algorithms for complex 3D imaging. To the best of the author's knowledge, no research has systematically investigated the application of CA for planar SM except [19-22]. This and upcoming work aims to examine the state of CA imaging and develops some of the theory of its application to breast tumour imaging. The main advantages of this approach, is that a standard clinical gamma camera is utilized that combines image quality, affordability and ease of use and potentially reduces the need for dedicated breast camera instrumentations. This is an attractive option for health care providers with limited resources where investment in single-application dedicated instrumentation is unattractive.

In this paper and the subsequent proposed approach, a planar single photon imaging gamma camera is used after replacing the conventional collimator with a planar MURA CA. The major anticipated advantages and motivations, first, CA imaging is well suited for detecting faint pseudo-point like objects in non-zero background. Imaging point-like small lesions (objects) in medicine is akin to imaging stellar points (objects) in astronomy. Thus, CA imaging appears well matched to the imaging objectives in SM. Theoretically, the selected CA patterns have wide open area and thus about half of the incident gamma-rays will be transmitted. This may dramatically improve the photon collection efficiencies and thus may reduce the acquisition time of the imaging system compared to a collimator based system. Combining CAs using geometric magnification with a full size standard gamma camera for imaging a relatively small organ such as breast has a potential ability to maintain the resolution compared to using a conventional collimator. In addition, the hole size of the mask dominates the spatial resolution, making the CA camera very attractive for early breast tumour imaging. Ultimately, high resolution could be achieved without the need for dedicated high resolution gamma camera instrumentations. In CA imaging photons impinging at a wide variety of angles are usually accepted, compared to the restricted angular acceptance when using collimator. This is because each hole of the CA provides a different view of the source object. Thus, inherent depth information contained in the data may be used to reconstruct a particular depth in the source object. This is achieved by re-scaling the magnification factor to the desired depth. This gives 3D information (limited angle tomography) from a single

conventional 2D image. Displacing the gamma camera away from the breast may allow access to a larger FoV. Thus, one possible application of CA-SM may be determining lymph node involvement. In addition, this may help in monitoring the tumour response to chemotherapy and may use for post-surgery and post chemotherapy applications. The use of CAs to replace the collimator minimizes the effects of camera-associated scatter as the surface area presented to the scatter flux is dramatically reduced (although, the patient scatter flux may be enhanced without appropriate shielding). Thus, CA imaging appears to be attractive for SM applications as it utilizes a limited, well-defined FoV, and the targets are "high" intensity point-like objects (lesions) which CA imaging methods are well suited to image.

In summary this paper has aimed at providing an appreciation of the diagnostic techniques of breast tumour imaging, discussing the relative merits of each of the current techniques highlighting the role of NM techniques as a unique tool for the in vivo investigation. Moreover, the motivations associated with CA imaging is also introduced emphasizing its possible attractive application in SM.

CONCLUSION

In summary, the main advantages of CA imaging systems are the high photon transmission, image magnification and to a lesser extent the (limited-angle) tomographic capability. The URAs and MURAs CA patterns have more attractive features compared to other patterns providing a δ like autocorrelation function of the imaging system. These properties have attracted the medical imaging community to renewed interest in the CAs imaging technique for breast tumour image. The increase in the resolution of imaging detectors as well as the increase in computing power and speeds have made this possible. In fact, multiple pinholes camera, MURAs and NTH-T-MURAs are the most widely used devices in the current nuclear medicine research [18-22]. Based on the author's opinion the URAs, MURAs and NTH-T-MURAs CA patterns of squares arrays expected to produce superior decoded images when used in breast tumour imaging applications. This is because the technique is ideal for imaging small isolated sources and thus provides a good match to the imaging objective of scintimammography.

FUTURE WORK

Future work will provide a description to the theoretical tools and the two methods used for investigating the application of CA for breast tumour imaging. The first method will base on the well-known MCS approach. The effects of limiting energy and spatial resolution are also will also be considered in the simulation for implementation of CA patterns and the basic

mask design and describing the other two methods used specifically for CA imaging investigations.

In addition to describes the various investigations undertaken using the proposed CA masks coupled to the gamma camera, starting with an idealized point source in air and then in tissue equivalent material. The complexity of the source geometry is increased to finally explore different extended object sizes as well as anthropomorphic torso phantoms. After the text edit has been completed, the paper is ready for the template. Duplicate the template file by using the Save As command, and use the naming convention prescribed by your conference for the name of your paper. In this newly created file, highlight all of the contents and import your prepared text file. You are now ready to style your paper; use the scroll down window on the left of the MS Word Formatting toolbar.

ACKNOWLEDGMENT

This Project was funded by the National Plan for Science, Technology and Innovation (MAARIFAH), King Abdulaziz City for Science and Technology, Kingdom of Saudi Arabia, Award Number (2516).

REFERENCES

1. Brown C., "Multiplex imaging with multiple pinhole camera", Journal of Applied Physics 45, 4, 1806-1810, 1974.
2. Fenimore E.E., and Cannon T.M., "Coded aperture imaging with uniformly redundant array", Applied Optics, 17, 3, 337-347, 1978.
3. Fenimore E.E., and Cannon T.M., "Uniformly redundant arrays", Proceeding Digital Signal Processing Symposium, 6, 7, 479-493, 1977.
4. Accorsi R.F., and Lanza R.C., "Near-field artifact reduction in coded aperture imaging", Applied Optics 40, 26, 4697-4705, 2001.
5. Mertz L., and Young N.O., "Fresnel Transformation of Image", Proceeding International Conference Optical Instrumentation, Chapman & Hall, London, 305-312, 1961.
6. Barrett H.H. and Swindell W., Radiological imaging: the theory of image formation, detection and Processing, London, Academic Press, Inc, ISBN: 0-12-079601-5, 1981.
7. Barrett H.H., "Fresnel Zone Plate Imaging in Nuclear Medicine", Journal of Nuclear Medicine, 4, 6, 382-385, 1972.
8. Rogers W.L., Han K.S., Jones L.W., Beierwaltes W.H., "Application of a Fresnel zone plate to -ray imaging", Journal of Nuclear Medicine, 13, 8, 612-615, 1972.
9. Fenimore E.E., Cannon T.M., and Miller E.L., "comparison of Fresnel zone plates and uniformly redundant arrays", SPIE, 149, 232-236, 1978.

10. Dicke R.H., "Scatter-hole Cameras for X-rays and gamma Ray", *Astro-physical Journal*, 153, 2, L101-L106, 1968.
11. Ables J.G, "Fourier transform photography: a new method for X-ray astronomy", *Proceedings of the Astronomic Society of Australia*, 1, 4, 172-173, 1968.
12. Busboom A., Elder-boll H., and Schotten H.D., "Uniformly redundant arrays", *Experimental Astronomy*, 8, 97-123, 1998.
13. Golay M.J.E., "Point arrays having compact, nonredundant autocorrelations", *Journal of the Optical Society of America*, 61, 272, 1971.
14. Gourlay A.R., and Stephen J.B., "Geometric coded apertures", *Applied Optics*, 22, 24, 4042-4047, 1983.
15. Gourlay A.R., and Young N.G., "Coded aperture imaging: a class of Flexible mask designs", *Applied Optics*, 23, 22, 4111-4117, 1984.
16. Gourlay A.R., Stephen J.B., and Young N.G., "Geometrically designed coded aperture masks", *Nuclear Instruments and Methods in Physics Research A*, 221, 54-55, 1984.
17. Gottesman, S.R., and Fenimore, E.E., "New family of binary arrays for coded aperture imaging", *Applied Optics*, 28, 4344-4352, 1989.
18. Meikle S.R., Fulton R.R., Eberl S., Dahlbom M., Wong K. and Fulham M.J., "An investigation of coded aperture imaging for small animal SPECT", *IEEE Transactions on nuclear science*, NS-48, 3, 816-821, 2001.
19. M. A. Alnafea, K. Wells, N. M. Spyrou, M. I. Saripan, M. Guy and P. Hinton, "Preliminary results from a Monte Carlo study of breast tumour imaging with low energy high-resolution collimator and a modified uniformly-redundant array-coded aperture", *Nuclear Instrument and Method A* 563:146-149, 2006.
20. M. A. Alnafea, K. Wells, N. M. Spyrou and M. Guy, "Preliminary Monte Carlo study of coded aperture imaging with a CZT gamma camera system for scintimammography", *Nuclear Instrument and Method A* 573:122-125, 2007.
21. M. A. Alnafea, D. Mahboub and K. Wells, "Non-Monte Carlo Methods for Investigating the Application of Coded Aperture Breast Tumour Imaging", *J Cancer Sci Ther* 2017, 9:12.
22. M. A. Alnafea and K. Wells "Monte-Carlo Simulation of Infinia Gamma Camera: A Verification and Validation Process" *Nessa J Cancer Sci and Therapy*, Volume 1, Issue 7, 1-14, January 2018.
23. Webb S., *The Physics of Medical Imaging*, Institute of Physics Publishing, Bristol and Philadelphia. ISBN: 0-85274-349-1, 1988.

24. Fenimore E.E., and Cannon T.M., "Uniformly redundant arrays: digital reconstruction methods", *Applied Optics*, 20, 10, 1858-1864, 1981.
25. Fenimore, E.E., "Coded aperture imaging: predicted performance of uniformly redundant array", *Applied Optics* 17, 22, 3562-3570, 1978.
26. Cannon T.M., and Fenimore E.E., "Tomographic Imaging Using Uniformly Redundant Arrays", *Applied Optics* 18, 7, 1052-1057, 1979.
27. Dunphy P., McConnell M., Owens A., Chupp E., Forrest D., and Googins J., "A balloon-borne coded aperture telescope for low-energy gamma-ray astronomy", *Nuclear Instruments and Methods in Physics Research Section A*, 274, 362-379, 1989.
28. Gemmill P.E., Chaney R.C., and Fenyves E.J., "Monte-Carlo simulation of a coded aperture SPECT apparatus using uniformly redundant arrays", *Imaging detectors in high energy and astroparticle physics*, Los Angeles, CA, Singapore, 81-115, 1995.
29. Zhang L., Lanza R.C., Horn B.K.P., and Zimmerman R.E., "Three-dimensional coded aperture techniques in diagnostic nuclear medicine imaging". *SPIE Conference on Physics of Medical Imaging*, 3336, 364-373, 1998.

AJMHR is

- Peer reviewed
- Monthly
- Rapid publication
- Submit your next manuscript at

info@ajmhr.com

